HHS Public Access

Author manuscript

Sci Transl Med. Author manuscript; available in PMC 2016 July 22.

Published in final edited form as:

Sci Transl Med. 2015 July 22; 7(297): 297ra116. doi:10.1126/scitranslmed.aab1482.

Inhibition of the alternative complement pathway preserves photoreceptors after retinal injury

J. Harry Sweigard[1], **Hidetaka Matsumoto**[1], **Kaylee E. Smith**[1], **Leo A. Kim**[2], **Eleftherios I. Paschalis**[2], **Yoko Okonuki**[1], **Alexandra Castillejos**[1], **Keiko Kataoka**[1], **Eiichi Hasegawa**[1], **Ryoji Yanai**[1], **Deeba Husain**[1], **John D. Lambris**[3], **Demetrios Vavvas**[1], **Joan W. Miller**[1], and **Kip M. Connor**[1,*]

[1]Angiogenesis Laboratory, Department of Ophthalmology, Massachusetts Eye and Ear Infirmary, Harvard Medical School, 243 Charles Street, Boston, MA 02114, USA

[2]Schepens Eye Research Institute, Massachusetts Eye and Ear Infirmary, Harvard Medical School, Boston, MA 02114, USA

[3]Department of Pathology and Laboratory Medicine, University of Pennsylvania, Philadelphia, PA 19104, USA

Abstract

[*]Corresponding author. kip_connor@meei.harvard.edu.

Author contributions: K.M.C. contributed to the study conception and design; J.H.S., H.M., K.E.S., and Y.O. performed RD surgery, immunohistochemistry, and quantification. J.H.S., K.E.S., and E.H. performed RT-PCR and ELISA assays. J.H.S., E.I.P., and R.Y. performed oxygen studies and associated immunohistochemistry. A.C. performed in situ hybridization. K.E.S. and K.K. did cell culture–related experiments. K.M.C. oversaw all research-related experiments. L.A.K. obtained the patient vitreous samples. J.D.L. and D.V. contributed new reagents/analytical tools. J.H.S., K.E.S., D.H., E.I.P., A.C., J.D.L., D.V., J.W.M., and K.M.C. contributed to the analysis and interpretation of the data. J.H.S., K.E.S., and K.M.C. wrote the paper.

Competing interests: Massachusetts Eye and Ear Infirmary holds a patent application on anti-complement therapeutics in ocular cell death titled “Methods of Preventing or Reducing Photoreceptor Cell Death” (PCT/US2014/059550), of which K.M.C. is an inventor. Additionally, Massachusetts Eye and Ear Infirmary has a proprietary interest in photodynamic therapy for conditions involving unwanted ocular neovascularization and has received financial remuneration related to this technology. J.W.M. receives a share of the same in accordance with institutional guidelines. J.W.M. is a named inventor on patents/patent applications on unrelated methods and compositions for preserving photoreceptor viability. In the past 36 months, J.W.M. has consulted for Alcon (serving on the Alcon Research Council); Biogen Idec Inc.; Amgen Inc.; Imagen Biotech Inc.; ISIS Pharmaceuticals Inc.; KalVista Pharmaceuticals, Ltd.; MacuLogix Inc.; ONL Therapeutics, LLC; and Regeneron Pharmaceuticals Inc. J.D.L. is the inventor of a patent and/or patent applications that describe the use of complement inhibitors for therapeutic purposes and is the founder of Amyndas Pharmaceuticals, which is developing complement inhibitors for clinical applications. J.D.L. consults for Achillion Pharmaceuticals, Baxter RA Pharmaceuticals, and ViroPharma. The other authors declare no competing interests.

SUPPLEMENTARY MATERIALS

www.sciencetranslationalmedicine.org/cgi/content/full/7/297/297ra116/DC1

Materials and Methods

Table S1. Human patient data for ELISA samples.

Fig. S1. Human samples of RD.

Fig. S2. Mouse model of RD.

Fig. S3. Complement expression in the mouse RD model.

Fig. S4. *Cd55* and *Cd59* are down-regulated in the detached retina.

Fig. S5. Outer nuclear layer expression of complement regulator *Cd55*.

Fig. S6. Expression of several key complement proteins after RD.

Fig. S7. The role of the lectin and classical complement pathways in outer nuclear layer cell death after RD.

Fig. S8. *Cd55* and *Cd59* are down-regulated in a photoreceptor cell line during hypoxia, and increasing serum concentrations cause MAC formation.

Fig. S9. Hypoxia makes photoreceptors more susceptible to complement-mediated cell death. References (59, 60)

Degeneration of photoreceptors is a primary cause of vision loss worldwide, making the underlying mechanisms surrounding photoreceptor cell death critical to developing new treatment strategies. Retinal detachment, characterized by the separation of photoreceptors from the underlying retinal pigment epithelium, is a sight-threatening event that can happen in a number of retinal diseases. The detached photoreceptors undergo apoptosis and programmed necrosis. Given that photoreceptors are nondividing cells, their loss leads to irreversible visual impairment even after successful retinal reattachment surgery. To better understand the underlying disease mechanisms, we analyzed innate immune system regulators in the vitreous of human patients with retinal detachment and correlated the results with findings in a mouse model of retinal detachment. We identified the alternative complement pathway as promoting early photoreceptor cell death during retinal detachment. Photoreceptors down-regulate membrane-bound inhibitors of complement, allowing for selective targeting by the alternative complement pathway. When photoreceptors in the detached retina were removed from the primary source of oxygen and nutrients (choroidal vascular bed), the retina became hypoxic, leading to an up-regulation of complement factor B, a key mediator of the alternative pathway. Inhibition of the alternative complement pathway in knockout mice or through pharmacological means ameliorated photoreceptor cell death during retinal detachment. Our current study begins to outline the mechanism by which the alternative complement pathway facilitates photoreceptor cell death in the damaged retina.

INTRODUCTION

Retinal detachment (RD) is one of the most common causes of photoreceptor cell death worldwide (1). It occurs either as a result of blunt trauma or as a side effect of a variety of diseases, including retinopathy of prematurity, diabetic retinopathy (tractional RD), ocular tumors, and age-related macular degeneration (exudative RD) (2–4). The current standard of care involves surgical reattachment through the use of pneumatic retinopexy, scleral buckle, and/or vitrectomy, which is typically provided within a week in the United States and Europe (5). Although surgery has proven to be highly effective at reattaching the retina, speed is critical to a positive outcome. This is because increased height and duration of the detachment results in a significant decrease in overall visual outcome (6). Unfortunately, even when reattachment is performed in a timely manner, patients often complain of permanent vision loss accompanied by changes in color vision (7–9). Visual acuity only improves to 20/50 in 39% of patients, even when early re-attachment surgery is performed (10, 11). Studies in both humans and animal models have shown that photoreceptor cell death is induced as early as 12 hours after RD (4, 12). This indicates that early intervention could potentially preserve the photoreceptors, improving the visual acuity of patients who undergo both early- and late-stage reattachment procedures. Currently, our knowledge of the processes for which photoreceptors degenerate is very poorly understood. Therefore, the first step to develop an effective therapeutic agent is to determine the underlying disease mechanisms to identify the most appropriate means for intervention.

One of the few known mechanisms regarding photoreceptor degeneration in RD is that the final degenerative events are apoptosis and necrosis (3, 4, 13). In either case, the early steps in the apoptosis and necrosis pathways involve events including the degradation of DNA

such that the cells are likely irreversibly compromised. Therefore, it becomes apparent that preventing the induction of death pathways is critical for preserving the integrity of the photoreceptors. Although we have a reasonable understanding of the intracellular signaling cascades for each cell death pathway, it remains unclear what the initial "trigger" is that induces cell death in RD. Evidence from the vitreous of patients with RD indicates the up-regulation of inflammatory mediators (4). Of particular interest are those belonging to the complement system (4). The complement system, part of innate immunity, has been shown to initiate cell death pathways in a number of disease models including acute lung injury (14), myocardial perfusion injury (15), and renal ischemia reperfusion (16). Thus, blocking complement may be a means to prevent entry of injured photoreceptor cells into the terminal stages of cell death.

The complement system represents a major component of immunity, playing a vital role in the defense against infection and in the modulation of immune and inflammatory responses (17–20). In addition to the well-established actions of complement in the elimination of pathogens, the complement system has been recently implicated in a variety of pathophysiological processes, including ischemia/reperfusion injury, sepsis, stroke, autoimmunity, inflammatory disorders, and inhibition of neovascularization (17, 21–24). Consisting of serum and tissue proteins, membrane-bound receptors, and regulatory proteins, the complement system is a hub-like network that is tightly connected to other systems. The complement system is composed of three pathways (classical, lectin, and alternative), each of which leads to the activation of the central complement component 3 (C3); subsequent entry into a final terminal pathway results in the formation of a nine-protein, 1-MD C5b-9 membrane attack complex (MAC), which forms a pore in the cell membrane to facilitate cellular clearance (17, 19, 25). Evolutionarily, the alternative complement pathway is the oldest of the complement activation pathways (17). Within the ocular microenvironment, the alternative complement cascade is under a continuous low-level state of activation, termed "tick-over," which allows for this pathway to have crucial immune surveillance functions (17). This constant level of activation ensures the intermittent probing of host self cells (17). Soluble and cell-bound regulators of complement (for example, Crry/CD46, CD55, and CD59) help to protect healthy host tissue from self-recognition and serve to prevent activation of a complement response (17, 26, 27). However, damaged or diseased host cells have been shown to down-regulate membrane-bound inhibitors of complement, allowing for targeted clearance (17, 28, 29). An imbalance between complement recognition and initiation on healthy host cells can lead to unregulated complement activation, opsonization, and/or subsequent cellular damage (17). Because of the constant tick-over of the alternative complement system providing immune surveillance, it would be ideally poised to rapidly respond to injury resulting from RD. We investigated whether the alternative complement pathway becomes activated in RD and whether its activation is detrimental to photoreceptor cell survival.

Here, we provide evidence that the alternative complement system is activated in patients with RD and use a mouse model of RD to provide mechanistic insight into the consequences of activation. We use a well-defined mouse model of RD, whereby a subretinal injection of sodium hyaluronate is used to create a detachment (13). The mouse RD model allows us to take advantage of well-established genetic manipulation in mice (for example, complement-

deficient knockout strains) to characterize the role of the alternative complement system. We show that in alternative pathway–deficient mice, the photoreceptors are protected from cell death. We next demonstrate that pharmacological inhibition of the alternative pathway significantly reduces photoreceptor cell death after RD in mice. These data suggest a role for complement in RD and that complement inhibition could protect photoreceptors in patients with RD (30).

RESULTS

The alternative complement pathway is activated in human patients with RD

The vitreous from patients with RD was assessed by enzyme-linked immunosorbent assay (ELISA) for the presence of complement factor B, a central regulator of the alternative pathway (table S1 and fig. S1, A and B) (31). Factor B was significantly up-regulated in RD patients ($P \leq 0.05$), indicating alternative pathway activation (Fig. 1A). There was no significant change in several other key complement proteins including factor D, complement component 5 (C5), and C3 (fig. S1, C to E). This is in line with previous studies that have shown that there are key regulatory proteins that undergo transcriptional control to modulate the activity of the complement pathways (31–33). For the alternative complement pathway, factor B has been described as a key effector molecule responsible for pathway activation (31).

The alternative pathway mediates photoreceptor cell death in a mouse model of RD

To define the role of the alternative complement pathway in RD, we used a mouse model that allowed us to take advantage of the genetic manipulation possible in mice (13). In this model, a sustained RD was created by a subretinal injection of 1% sodium hyaluronate, resulting in about 60% of the retina becoming detached (Fig. 1B) (13). Photo-receptor cell apoptosis was assessed from 12 to 72 hours after detachment by identifying TUNEL (terminal deoxynucleotidyl transferase–mediated deoxyuridine triphosphate nick end labeling)–positive cells in the outer nuclear layer (fig. S2, A to D). The peak amount of cell death occurred at 24 hours after detachment (fig. S2, C and D). We assessed factor B expression in the retinas of mice with or without RD and found significant up-regulation from 12 to 48 hours after detachment, peaking at 24 hours (Fig. 1C and fig. S3A; $P \leq 0.05$ to 0.0001). Key activators for the lectin (Masp2) and classical (C1q) complement pathways were also assessed, and in both cases, up-regulation was less than that found for the alternative pathway; however, there were some time points with minor alterations (fig. S3B).

Cd55 and *Cd59* expression is suppressed in response to RD

Soluble and cell-bound regulators of complement help to protect healthy host tissue from self-recognition, providing protection from erroneous activation(34–37). However, damaged or diseased host cells have been shown to down-regulate membrane-bound regulators of complement, allowing for their targeted clearance (28, 38–40). We assessed the expression of several genes encoding key cell-bound regulators known to play a role in the retina, including *fH*, *Crry*, *properdin*, *Cd59*, and *Cd55*. We found that *Cd55* and *Cd59*, key regulators of the alternative pathway (36), were significantly down-regulated in the detached retina (Fig. 1C; $P \leq 0.05$ to 0.0001), making these cells intrinsically more prone to targeted

cell death. To confirm that the decline in *Cd55* and *Cd59* was specific to the photoreceptors, we performed in situ hybridization. A comparison of the attached and detached regions of the retina from the same eye revealed that *Cd55* and *Cd59* expression was down-regulated in the detached area (Fig. 1, D and E, and fig. S4). Additionally, we isolated the outer nuclear layer using laser capture microdissection (fig. S5, A to C) and assessed gene expression by real-time polymerase chain reaction (RT-PCR) for *Cd55*. *Cd55* expression in the photoreceptors was significantly reduced (74.6 ± 5.262%; $P \leq 0.0001$) in response to RD (fig. S5A). Retinal expression of *fH*, *Crry*, and *properdin* was not significantly altered, with the exception of *Crry* and *properdin* at 12 hours after RD, suggesting cell type specificity for individual complement regulatory proteins (fig. S6, A to C; $P \leq 0.01$). In RD, the photoreceptors appear to be highly susceptible to alternative pathway–mediated cell death due in part to down-regulation of key complement regulators.

Alternative pathway–deficient mice are protected from RD-associated photoreceptor cell death

Photoreceptor cell death in response to RD was next assessed in a $C3^{-/-}$ mouse, which lacks the central C3 protein required for all three complement pathways (17). Photoreceptor cell death was quantified at 24 hours after detachment, the peak of cell death. $C3^{-/-}$ knockout mice showed a reduction in the number of TUNEL-positive cells compared to age- and strain-matched controls (Fig. 2, A and B). To further define the role of C3 in RD, C57Bl6 (control wild-type) mice were given injections of an immunoprecipitating antibody (Ab) against C3 in the subretinal space at the time of detachment. Quantitation of TUNEL labeling revealed that administration of an anti-C3 Ab significantly protected the mice from photoreceptor cell death in response to RD compared to an isotype-matched control Ab (Fig. 2, C and D; $P \leq 0.01$ and $P \leq 0.0001$, respectively). Conversely, we used the opposite approach whereby we reactivated complement in $C3^{-/-}$ mice by introducing cobra venom factor, which is a stable functional analog of C3b (41). This bypasses the need for C3 by replacing the C3 cleavage product, C3b, with a functional analog required for the alternative pathway proteolytic cascade to continue. Typically, cobra venom factor is used in immune studies for its ability to deplete complement systemically through rapid, sustained activation of the complement system, exhausting the available circulating complement proteins. Here, we took advantage of its ability to “activate” complement by delivering cobra venom factor locally to the ocular environment of the $C3^{-/-}$ mice. The reactivation of the complement system in $C3^{-/-}$ mice using cobra venom factor increased photoreceptor cell death after RD compared to that of $C3^{-/-}$ mice that received a phosphate-buffered saline (PBS) control injection (Fig. 2, E and F). Together, these results strongly implicate the complement system as a driving force in promoting the early photoreceptor cell death associated with RD.

The alternative complement pathway remains in a primed state through constant tick-over of the central C3 protein, which allows for continuous probing within the retinal microenvironment [and central nervous system (CNS)] for the identification of cells that are damaged or dying, distinguishing the alternative pathway from the lectin and classical pathways (17, 42). To determine the role of the alternative pathway in photoreceptor cell death during RD, we tested mice that lacked factor B ($Fb^{-/-}$), an essential rate-limiting protein required for alternative pathway activation after C3 cleavage (31). Mice deficient in

the alternative complement pathway ($Fb^{-/-}$) showed a substantial decrease in photoreceptor cell death 24 hours after RD (Fig. 3, A and B). Complement factor D is a serine protease that cleaves factor B once bound to C3b, resulting in the assembly of the alternative pathway C3 convertase (17). To pharmacologically block the alternative complement pathway in RD, we injected an immunoprecipitating Ab against factor D into the subretinal space of C57Bl6 control mice at the time of detachment. Inhibition of factor D resulted in a reduction in the amount of photoreceptor cell death compared to mice treated with an isotype-matched Ab control (Fig. 3, C and D). Notably, knockout mice deficient in either lectin *Mbl A*/$C^{-/-}$ or classical $C1q^{-/-}$ pathways did not confer protection against complement-mediated photoreceptor cell death (fig. S7, A to D). These data suggest that the alternative complement pathway, and not the lectin or classical pathways, mediates photoreceptor cell death in response to RD.

Retinal hypoxia leads to alternative pathway activation and cell death in RD

Photoreceptor cells are one of the most highly metabolic cell types in the body (43). However, with such high metabolic demand, they are not permeated with a vascular network, deriving 90% of their nutrients and oxygen by diffusion from the vascular bed of the choroid/choriocapillaris (43, 44). When RD occurs, it physically separates the photoreceptor cells from the retinal pigment epithelium and distances these cells from the choroid, thereby compromising access to nutrients and oxygen. Several seminal studies have shown that oxygen deprivation (hypoxia) is a leading cause of photoreceptor cell death in RD (45, 46). With this in mind, we tested whether hypoxia could facilitate alternative complement pathway activation and photoreceptor cell death in response to RD. To define global hypoxia in photoreceptors in response to RD, we injected mice 22.5 hours after detachment intra-peritoneally with a marker of hypoxia called Hypoxyprobe. Hypoxyprobe is a thiol-binding probe that only binds to cells with an oxygen concentration less than 14 μM, which can be visualized through 3,3′-diaminobenzadine amplification. We enucleated the eyes of the mice with RD 1.5 hours after injecting Hypoxyprobe and prepared cross sections. In sections where half of the retina was detached and the other half remained attached, we only observed Hypoxyprobe binding in the detached region of the outer nuclear layer (Fig. 4A). To obtain a more precise reading of the retinal oxygen concentration in vivo, we used a glass oxygen microsensor containing a silicone membrane that allows for the diffusion of oxygen into an oxygen-reducing cathode. Placing the probe into the attached retina using a stereotactic frame, we defined an average oxygen concentration of 47.64 ± 3.35 μM compared to the contralateral detached retina with an average oxygen concentration of 17.14 ± 5.03 μM (Fig. 4B). To assess whether the hypoxic state of the photoreceptors facilitated alternative pathway–mediated cell death, we analyzed RD in mice housed in room air (21% oxygen) or housed in a chamber maintained at 75% oxygen. After 24 hours, we enucleated the eyes and performed TUNEL labeling. Quantitation of TUNEL-positive cells in the outer nuclear layer revealed a significant reduction in cell death within the group of mice maintained at 75% oxygen (Fig. 4, C and D; $P \leq 0.0001$). The mice kept in 75% oxygen had less expression of factor B than those kept in room air (Fig. 4E), indicating an oxygen-dependent regulation of factor B. To confirm that complement activation led to MAC-mediated cell death, we used a photoreceptor cell line (661W) under hypoxic conditions and added serum (a key source of complement) to activate the complement

cascade. We found that 661W cells kept under hypoxic conditions (1% O_2) showed decreased expression of both *Cd55* and *Cd59* (fig. S8, A and B), which was sufficient to lead to increased MAC deposition (fig. S8C) and, ultimately, 661W cell death (Fig. 4F and fig. S9, A and B). Together with the previous data from $C3^{-/-}$ and $Fb^{-/-}$ mice, this indicates that alternative pathway activation is required for cell death and that hypoxia participates in the stimulus to promote complement activation. This is in accord with previous work showing that hypoxia leads to complement activation and deposition of iC3b, causing an intracellular signaling cascade that results in the formation of reactive oxygen species and, ultimately, cell death (47).

DISCUSSION

We have found that human patients with RD have increased expression of factor B, indicating alternative pathway activation (Fig. 1A and fig. S1). We do not see a change inC3, C5, or factor D, corroborating previous reports that factor B is the key rate-limiting protein in alternative pathway activation (32). Of the three arms of complement (classical, lectin, and alternative), factor B is exclusive to the alternative pathway. An increase in expression of *Fb*, the gene encoding factor B, leads to the formation of a C3 convertase that amplifies the pathway by cleaving the C3 protein, central to the alternative pathway. Ultimately, alternative pathway activation proceeds to MAC formation, lysing cells by forming a lytic pore on the cell membrane. To gain mechanistic insight into the increased expression of factor B seen in our human patient samples, we used a mouse model of RD. In this model, increased *Fb* expression peaked with photoreceptor cell death (Fig. 1C and figs. S2C and S3A) at 24 hours. At the same time, there was a decrease in *Cd55* and *Cd59* expression (negative regulators of the alternative pathway), making the photoreceptors prone to complement-mediated attack (Fig. 1, C to E). Mice in which the central C3 protein of the alternative pathway was missing ($C3^{-/-}$) or inhibited were protected from photoreceptor cell death (Fig. 2, A to D), and reactivation of the pathway was sufficient to restore the injury phenotype (Fig. 2, E and F). We further confirmed the role of the alternative pathway using mice that lacked factor B ($Fb^{-/-}$) and found a similar reduction in the amount of photoreceptor cell death (Fig. 3).

The height and duration of RD are critical determinants for the degree of vision loss associated with RD (6) due to the reliance of the photoreceptors on the diffusion of nutrients from the choroidal vasculature (6, 46). Previous studies have elegantly shown that the hypoxia associated with RD is linked to photoreceptor cell death (46, 48, 49). Our work expands on these findings by providing a mechanism for how hypoxia can in part induce photoreceptor cell death through alternative pathway activation. The down-regulation of *Cd55* and *Cd59* in the photoreceptor cell layer would make the cells susceptible to alternative pathway–mediated lysis. We observed that cell death in the outer nuclear layer occurs in clusters rather than in a uniform pattern. One possibility for this pattern is that complement activation led to the initial lysis of a subset of cells and subsequent release of their intracellular components, which triggered neighboring cells to undergo programmed cell death by apoptosis. The observed cell death was highly restricted to the outer nuclear layer, and at this point, we do not know how the other cell layers were protected. One possibility is that the other cell layers did not become hypoxic. The superficial retinal

vasculature of the ganglion cell layer and deep retinal vasculature of the inner nuclear layer may supply sufficient nutrients and oxygen to prevent complement inhibitor down-regulation in these layers. Additionally, it is possible that the retinal cell layers express different complement inhibitor profiles that are not susceptible to hypoxic regulation.

Whereas we have found that the alternative pathway is playing a profound role in photoreceptor cell death associated with RD, several key questions remain. The essential rate-limiting protein factor B is up-regulated in response to RD; however, currently, we do not know the cellular source of complement in the retina. Macrophages are known to produce high levels of factor B when they become activated (50, 51) and therefore could be the source. Another possibility is that the resident microglia are responding to the initial insult by producing factor B and depleting C3, subsequently recruiting circulating macrophages to the retina. Support for this idea comes from a study performed using a light-induced model of retinal degeneration that shows peak cell death in the outer nuclear layer at 24 hours and peak C3 expression at 7 days (52). In that study, the authors suggest the possibility of infiltrating macrophages contributing to C3 production. This raises the intriguing possibility that there may be temporal changes in expression where microglia initiate the alternative pathway by expressing factor B and at the same time recruit macrophages. The macrophages then migrate into the retina and produce C3. In our study, we focused on an early time point to determine the initiating events and to see peak cell death corresponding to peak factor B expression. It would be interesting to see whether C3 expression increased at a later time point in the RD mouse model, similar to what has been reported in the light-induced model. In addition, it has been shown that microglia isolated from aged mice tend to produce an increase in both factor B and C3 (53), indicating that resident microglia are capable of producing essential alternative pathway components. It would be beneficial to tease out the distinct functions of microglia and macrophages in RD.

We observed a marked reduction in *Cd55*/*Cd59* in photoreceptors, making them exceptionally prone to opsonization and hence strongly chemoattractive for macrophages. It has also been shown that Müller cells become activated during RD, producing a variety of growth factors and changing their profile of Toll-like receptor expression (54–56). Therefore, Müller cells could be a first responder to the physical separation of the retina, thereby recruiting peripheral macrophages or local microglia to the site of detachment. Examining the response and time course of local microenvironmental changes and the migration of circulating macrophages to the site of detachment could lend further mechanistic insight into the inflammatory process. Another question that remains is how *Cd55* and *Cd59* become down-regulated in the photoreceptors. Our previous work indicated that endothelial cells down-regulate *Cd55* in response to hypoxia (28). Here, we show using 661W cells that photoreceptor cells can also directly respond to hypoxia by down-regulating *Cd55* and *Cd59* (fig. S8). Whereas this begins to answer how photoreceptors become vulnerable to complement-mediated attack, subsequent in vivo studies linking complement expression changes in cell types of interest (Müller cells, microglia, and photoreceptors) will provide a more complete understanding of how the cells within the retinal microenvironment communicate during trauma.

We propose a mechanism whereby the physical separation/hypoxic state of the retina in part leads to Cd55 and Cd59 down-regulation (essential complement regulatory proteins) in the photoreceptors with a concomitant rise in factor B, which results in targeting of the photoreceptors for complement-mediated cell lysis. There is increasing evidence suggesting that a delicate balance of complement pathway activity can be valuable for CNS tissue homeostasis (28, 57). Here, we have shown how a specific cell type, the photoreceptors, can be negatively affected through modulation of complement pathway activators and inhibitors. RD is a sight-threatening complication in some of the most common forms of blindness, such as age-related macular degeneration and diabetic retinopathy. In addition, RD can be caused by blunt trauma such as military blasts or sports injuries. The delay between when the patient presents at the clinic to the scheduled surgery, generally 7 to 10 days, can often lead to permanent vision loss. Understanding the mechanism behind the disease may allow clinicians to inject a drug into the eye at the time of diagnosis to slow or prevent photoreceptor cell death until the RD can be surgically repaired. However, there are some limitations to our study. For example, anti-complement Ab administration was given subretinally at the time of detachment, whereas in a clinical setting, most drugs are administered intravitreally at the time of presentation. This lag time from the initial detachment to therapeutic anti-complement Ab treatment could result in significant photoreceptor cell loss. Moreover, retinal penetration and efficacy may vary with intra-vitreal injections compared to subretinal injections. Also, our animal model of RD is acute, and peak cell death occurs within 24 hours, making treatment after detachment difficult to assess. Furthermore, our animal model of RD does not completely recapitulate clinical rhegmatogenous RD because no retinal tear occurs in our model. The role of retinal tear on complement induction and photoreceptor hypoxia/cell death is currently unknown. Nevertheless, our work contributes to elucidating the therapeutic potential of emerging anti-complement therapies in RD and other diseases of retinal injury.

MATERIALS AND METHODS

Study design

The end goal of this study was to identify the role of the alternative complement pathway in RD and identify a mechanism by which it is activated. The vitreous from patients with RD versus a control cohort (macular hole or epiretinal membrane) was assessed for key components of the complement system by ELISA. We subsequently used a mouse model of RD, which provided a systematic and controlled system allowing us to take advantage of genetic manipulation possible in mice. All time points were assessed at 24 hours after detachment, the height of cell death in this model. In studies where the complement pathways were inhibited or reactivated, 1 μl of the compound assessed (cobra venom factor, anti–factor D, anti-C3, or vehicle control) was administered subretinally immediately before injecting the 1% sodium hyaluronate. Experimental groups were defined to allow for statistical analysis. Patient and mouse specimens were masked as to group identity and only unmasked after analysis.

Mouse model of RD

This study adhered to the Association for Research in Vision and Ophthalmology statement for the Use of Animals in Ophthalmic and Vision Research. C57Bl6 mice were obtained from The Jackson Laboratory (stock no. 000664). *Fb*$^{-/-}$, *C3*$^{-/-}$, and *C1q*$^{-/-}$ mice were a gift from J.D.L. at the University of Pennsylvania. *Mbl A/C*$^{-/-}$ were a gift from G. Stahl at Brigham and Women's Hospital. Each strain was maintained as a breeding colony in the Massachusetts Eye and Ear Infirmary animal facility and was between the ages of 8 and 12 weeks for all studies performed. The model of RD was performed as previously described (13).

Human vitreous

All human vitreous samples were obtained using a protocol approved by the Institutional Review Board at Massachusetts Eye and Ear Infirmary and de-identified/anonymized. Undiluted vitreous (0.3- to 1.0-ml volume) was obtained from patients during standard, three-port pars plana vitrectomy under direct visual control by aspirating liquefied vitreous from the center of the vitreous cavity with a syringe before starting the infusion. Vitreous was obtained from nine patients with varying degrees of RD and four patients who had a macular hole or epiretinal membrane with no RD (control samples) (table S1). Samples were kept on ice during the time of surgery and then immediately moved to −80°C for storage. To separate the soluble protein from the collagenous matrix, the samples were thawed on ice and then spun at 12,000 rpm for 15 min at 4°C (58). The supernatant was collected, aliquoted, and stored at −80°C. Each aliquot was not thawed more than once for use in the ELISA assays.

Statistical analysis

Values are expressed as means ± SEM (unless specified), and statistical analysis was performed using an unpaired Student's *t* test (****$P < 0.001$, ***$P < 0.001$, **$P < 0.01$, *$P < 0.05$; ns, $P > 0.05$).

MATERIALS AND METHODS

Mouse model of retinal detachment

This study adhered to the ARVO statement for the Use of Animals in Ophthalmic and Vision Research. C57Bl/6 mice were obtained from Jackson laboratories (stock number 000664). *Fb*−/−, *C3*−/−, and *C1q*−/− mice were a gift from Dr. John Lambris at the University of Pennsylvania. *Mbl A/C*−/− were a gift from Dr. Gregory Stahl at Brigham and Women's Hospital. Each strain was maintained as a breeding colony in the MEEI animal facility and were between the age of 8–12 weeks for all studies performed. The model of retinal detachment was performed as previously described (13). Briefly, mice were anesthetized using a mixture of ketamine (60mg/kg) and xylazine (6mg/kg). Deep anesthesia was confirmed by a toe pinch test. One drop of proparacaine hydrochloride (0.5%) (Akorn, 17478-263-12) was administered to each eye. Using a dissecting microscope an incision was made in the temporal conjunctiva to separate the conjunctiva from the sclera. A self-sealing scleral incision was made using the tip of a 30 G needle with the bevel pointed up and a

tunnel was made to penetrate the sclera into the choroid. The cornea was then punctured with a 30 G needle to reduce intraocular pressure. A 33 G needle connected to a Hamilton syringe was then inserted into the subretinal space with the bevel pointed down (towards the inner eye), and 3.5μl sodium hyaluronate was injected slowly to detach the neurosensory retina from the underlying RPE. To reduce the risk of sodium hyaluronate leakage cyanoacrylate surgical glue was placed on the scleral wound. Finally, the conjunctiva was reattached to its original position using cyanoacrylate surgical glue, further reducing the risk of sodium hyaluronate leakage. Mice were kept on a heating pad until fully awake, confirmed by upright mobility. This model varies somewhat from a previously reported mouse model of RD (57, 58) in that we use 3.5μl of Provisc®, as opposed to 1μl, and we seal the scleral cut with glue to prevent Provisc® leakage. These alterations likely make our model slightly more severe since it would result in an increased height of detachment.

Human vitreous

All human vitreous samples were obtained using a protocol approved by the Institutional Review Board at Massachusetts Eye and Ear Infirmary and de-identified/anonymized. Undiluted vitreous (0.3 to 1.0 mL volume) was obtained from patients during standard three-port pars plana vitrectomy under direct visual control by aspirating liquefied vitreous from the center of the vitreous cavity with a syringe before starting the infusion. Vitreous was obtained from 9 patients with varying degrees of retinal detachment (RD) and 4 patients that had a macular hole with no RD (control samples) (Supplemental table 1). Samples were kept on ice during the time of surgery then immediately moved to −80°C for storage. In order to separate the soluble protein from the collagenous matrix the samples were thawed on ice then spun at 12,000 RPM for 15 minutes at 4°C (59). The supernatant was collected, aliquoted, and stored at −80°C. Each aliquot was thawed not more than once for use in the ELISA assays.

ELISAs for measuring complement proteins

Human—All human ELISA measurements were performed using 5μl of undiluted vitreous, isolated as described above. All ELISAs were performed following kit instructions and measured using a Molecular Devices Spectramax M3 plate reader. Standard curves were generated using the standard reagents provided in the kit then sample values determined automatically using Softmax pro software. Human ELISA kits that were used include Fb (Novatein, BG-HUM10501), Fd (Abcam, ab99969), C5 (Abcam, 125963), and C3 (Abcam, ab108822).

Mouse—For mice Whole retinas were isolated and flash frozen in liquid nitrogen then stored at −80°C. Protein extraction was performed using M-Per protein extraction reagent (Thermo Scientific, 78501, Waltham, MA) and concentration determined using the Bradford assay. ELISAs for Fb (NovateinBio, BG-MUS10520) using retina were performed by following kit instructions and measured as described above.

RTPCR to measure complement activity

RNA was isolated using an RNeasy micro kit (Qiagen, 74004, Valencia, CA) for LCM samples or an RNeasy mini kit (Qiagen, 74106, Valencia, CA) for whole retina. Total RNA

was measured using a nanodrop spectrophotometer (Thermo Scientific, Nanodrop 2000, Waltham, MA) then each sample was normalized prior to transcribing cDNA. cDNA was transcribed using superscript III (Invitrogen, 18080-044, Carlsbad, CA) then one microliter of cDNA was used for each RTPCR reaction. Primers to Fb (Life Technologies, Mm004333909), C1q (Life Technologies, Mm00432142), MASP2 (Life Technologies, Mm00521963), Cd55 (Life Technologies Mm00438377), and Cd59a (Life Technologies, Mm00483149) were used for whole retina and combined with Taqman universal PCR master mix (Life tehcnologies, 4304437). Primers for Cd55 using photoreceptors isolated by LCM were obtained through Integrated DNA Technologies using their online Primer Quest design tool and importing the NCBI ID number for the sequence (Forward 5′-TGTAAGCAGAATCGCCACAGAGGT-3′ and Reverse 5′-GTGAGCTTCCACTGCAGGTTTGTT-3′). RTPCR was run in triplicate and the average of each CT value used for analysis. All CT values were normalized to beta actin from each sample as an internal control. Final values were determined using the ΔΔCT method.

TUNEL labeling and quantitation of dying cells in the ONL

Following RD treatment eyes were enucleated at the indicated time points. The eyes were frozen in OCT (Tissue Tek, 4583) using chilled isopropanol in dry ice with the glue spot (provisc injection site) facing down and 14μm sections were taken until the first sign of RD became evident. 4 sections were then taken with 75μm gaps between each section to span the RD. TUNEL labeling was performed using a Roche TUNEL kit (Roche, 12156792910) following the kit instructions. The sections were coverslipped with DAPI containing medium (Vector Labs, H-1200). Using the 40x objective a DAPI image was taken at the mid point from the optic nerve to the end of the retina for each half of the eye (Supplemental Fig. 2, red boxes). The DAPI image was then overlayed with an image of the texas red channel (TUNEL cells). Using the merged image in ImageJ the area of the ONL was outlined then the number of TUNEL positive cells overlapping with DAPI cells was counted. Regions from all 4 sections were averaged then graphed in Prizm.

Isolation of the ONL using laser capture micro-dissection

Eyes were enucleated 24 hours post RD then placed in OCT compound (Tissue Tek, 4583, Torrance, CA), and quickly frozen by submerging in a beaker of isopropanol chilled by dry ice. Between 16 and 18 sections cut at 30μm were placed onto a frame slide (leica 11505190, Germany) under RNAse free conditions then allowed to air dry for 10 minutes. All reagents were made using nuclease free water (Ambion, AM9932, Carlsbad, CA). The sections on the frame slides were fixed using a graded series of EtOH (Sigma, 459836-1L, St. Louis, MO) consisting of incubation in 50% EtOH for 1 minute, 75% EtOH for 1.5 minutes, and water for 1 minute. To identify the cell layers the slides were dipped in 0.1% toluidine blue solution (Fluka, 89640-5G, St. Louis, MO) followed by 2 rinses in water for 15 seconds each, 75% EtOH for 30 seconds, and water for 15 seconds. Sections were dried in room air then the photoreceptors were isolated using laser capture micro-dissection (Leica, LMD 7000, Germany). Samples were collected in RNAlater® solution (Ambion, AM7022, Carlsbad, CA) and stored at −80°C until RT-PCR was performed.

Complement blocking and re-activation studies in mice

C3 neutralizing antibody—In order to dampen complement activation a neutralizing antibody was injected against the central C3 protein required for complement amplification. Prior to *in vivo* injection the azide was removed from the C3 antibody (Abcam, ab11862) using an Abcam purification kit (ab102784) following kit instructions. Briefly, 200μl of C3 antibody was used for starting material and incubated in in the provided resin containing 20μl of 10x binding buffer for 1 hour at room temperature with gentle agitation. The resin was then spun to remove unbound antibody and washed with the provided wash buffer. The antibody was eluted with 100μl of elution buffer then 25μl of neutralizer was added. The elution procedure was repeated 3 times using separate collecting tubes. Only the first tube was used for *in vivo* injections corresponding to 0.1mg/ml. The model of retinal detachment was performed precisely as described above with one modification: Prior to injecting the provisc 1μl of the purified C3 antibody (0.1μg) or IgG2a isotype control (Life Technologies, 02-9688) was injected into the sub-retinal space through the scleral tunnel. The eyes were enucleated 24 hours after RD and processed for TUNEL labeling as described earlier.

Fd neutralizing antibody—To dampen the alternative pathway an antibody was injected that binds to Fd (R&D systems, MAB5430) prior to creating RD. The antibody did not contain azide therefore was resuspended in PBS to a final concentration of 0.5mg/ml, alliquoted, and stored in −20°C. The antibody was not thawed more than once for injection. The model of retinal detachment was performed precisely as described above with one modification: Prior to injecting the provisc 1μl of the purified Fd antibody (0.5μg) or IgG1 isotype control (Life Technologies, R100) was injected into the sub-retinal space through the scleral tunnel into the sub-retinal space. The eyes were enucleated 24 hours after RD and processed for TUNEL labeling as described earlier.

Re-activation of the complement system in *C3*$^{-/-}$ mice—To re-activate complement in *C3*$^{-/-}$ mice we injected 1μl (1.1mg) of cobra venom factor (CVF) (quidel, A600) into the sub-retinal space prior to the Provisc® injection. When introduced into the blood stream CVF activates complement, bypassing the need for endogenous C3. The rest of the model of retinal detachment was performed precisely as described above. The eyes were enucleated 24 hours after RD and processed for TUNEL labeling as described earlier.

Detecting hypoxic regions in the retina

Hypoxic areas of the retina were identified 24 hours after detachment with the use of the Hypoxyprobe™-1 Plus kit (HPI, HP2-100). Hypoxyprobe™ (pimonidazole hydrochloride) is a substituted 2-nitoimidazole that forms adducts with thiol containing proteins in only those cells that have an oxygen concentration less than 14μmol (ie. hypoxic cells). Retinal detachments were made as described above and 22.5 hours later mice were anesthetized with a mixture of ketamine (60mg/kg) and xylazine (6mg/kg) then injected with Hypoxyprobe™ (2mg in a volume of 100μl) directly into the left ventricle. Mice were kept on a heating pad maintained at 37°C and monitored for 90 minutes to allow complete binding of the probe to hypoxic tissues. The eyes were enucleated and frozen in OCT that had been chilled in dry ice. Blocks were sectioned at 20μm then fixed in 4%PFA for 20 minutes. The endogenous peroxidase present in the tissue was quenched using 3% H_2O_2 for

5 minutes. Non-specific binding was blocked using 5% fetal calf serum/0.5% triton x/0.3% bovine serum albumin. Samples were then incubated with a FITC conjugated mouse IgG1 that binds to pimonidizole (Hypoxyprobe™) at a dilution of 1:100. The FITC was amplified using rabbit anti-FITC conjugated with horseradish peroxidase at a dilution of 1:75 followed by the addition of a brown DAB chromagen. To identify the retinal layers slides were dipped in haematoxylin (Sigma, H9627) for 1 minute then washed 3 times in PBS and coverslipped. Binding of the probe was compared on retinal cross sections where 50% of the retina was attached and the other 50% detached.

Retinal oxygen measurements

In vivo oxygen measurements were performed using a 50μm diameter glass-electrode-oxygen sensor (Unisense A/S, Denmark). This probe has a linear response between 0–1 atm pO_2 ranges, negligible oxygen consumption (10–16 mol/sec) and fast time response. The cathode is polarized against an internal Ag/AgCl anode that results in rapid, 0.3 second, *in vivo* oxygen measurements. Prior to its use, the sensor was thoroughly pre-polarized for 24 hours and was calibrated using two points: maximum oxygen saturation using 0.9% saline at 37 °C under continuous air agitation, and zero oxygen calibration using sodium ascorbate solution. A linear fit was calculated from the two calibration points and implemented into the data acquisition software. Sampling rate was adjusted to 1Hz (Nyquist-Shannon sampling theorem) and measurements were acquired and stored in a portable computer for later processing.

Animal preparation—Mice were anesthetized by using a mixture of ketamine (60mg/kg) and xylazine (6mg/kg) administered via an intra-peritoneal (IP) injection. Adequate sedation was confirmed by toe pinch. One drop of proparacaine hydrochloride (0.5%) (Akorn, 17478-263-12) was administered to each eye. A stereotaxic frame (Leica 39463001) with Cunningham mouse adaptor (Leica 39462950) was used to immobilize the head of the mouse. A 32 gauge needle was then used to create a tunnel into the subretinal space. A manual (x,y,z) microstage, adapted with the oxygen sensor, was used to gently guide the probe into the subretinal space adjacent to the detached retina and measurements were performed for several seconds, until oxygen readings were stabilized. Oxygen measurements in the contralateral non-detached eyes served as internal controls and naïve mice served as control reference. During the experimental time frame the probe was retested for accuracy in the calibration solutions and found to be within range. The mice were euthanized by spinal dislocation after the final reading.

Supplementing oxygen after retinal detachment

Retinal detachments were performed as described above then the mice were kept either in the animal holding facility (≈21% O_2) or immediately placed into an oxygen chamber maintained at constant 75% O_2 (Biospherix model 110). After 24 hours the mice were anesthetized under a heavy dose of avertin (2,2,2 tribromo ethanol, Sigma, T4, 840-2) at a working concentration of 10mg/ml and injected at a dose of 0.25–0.5 mg/gram intraperitoneally. In one group the eyes were enucleated and frozen in OCT compound using isopropanol chilled by dry ice. The eyes were then processed for TUNEL labeling and

quantified as described above. In the other group the retina was removed and immediately flash frozen in liquid nitrogen for RNA extraction. All eyes were stored at −80°C.

Statistical analysis

Values are expressed as mean ± SEM (unless specified) and statistical analysis was performed using an unpaired Student t test (***: P<0.001, **: P<0.01, *: P<0.05, ns: P>0.05).

Supplementary Material

Refer to Web version on PubMed Central for supplementary material.

Acknowledgments

We thank G. Stahl (Brigham and Women's Hospital, Harvard Medical School) for providing the *Mbl A/C*$^{-/-}$ mice and M. Al-Ubaidi from the University of Oklahoma College of Medicine for use of the 661W photoreceptor cell line.

Funding: This study was supported by NIH grants R01EY022084–01/S1 (K.M.C.), EY020633-02 (J.D.L.), R21EY023079 (D.V.), 5K12EY016335 (L.A.K.), T32EY007145 (J.H.S.), and P30EY014104; Howe Laboratory endowment of the Massachusetts Eye and Ear Infirmary; March of Dimes Foundation grant no. 5-FY09-535; Research to Prevent Blindness (RPB) Special Research Scholar Award (K.M.C.), RPB Physician-Scientist Award (D.V.), and unrestricted grant (J.W.M.); Massachusetts Lions Eye Research Fund Inc.; Yeatts Family Foundation (D.V.); The Loeffler Family fund; 2013 Macula Society Research grant (D.V.); and an award from the Japan Eye Bank Association (R.Y.).

REFERENCES AND NOTES

1. Subramanian ML, Topping TM. Controversies in the management of primary retinal detachments. Int Ophthalmol Clin. 2004; 44:103–114. [PubMed: 15577567]
2. Day S, Grossman DS, Mruthyunjaya P, Sloan FA, Lee PP. One-year outcomes after retinal detachment surgery among medicare beneficiaries. Am J Ophthalmol. 2010; 150:338–345. [PubMed: 20591398]
3. Rowe JA, Erie JC, Baratz KH, Hodge DO, Gray DT, Butterfield L, Robertson DM. Retinal detachment in Olmsted County, Minnesota, 1976 through 1995. Ophthalmology. 1999; 106:154–159. [PubMed: 9917797]
4. Yu J, Peng R, Chen H, Cui C, Ba J. Elucidation of the pathogenic mechanism of rhegmatogenous retinal detachment with proliferative vitreoretinopathy by proteomic analysis. Invest Ophthalmol Vis Sci. 2012; 53:8146–8153. [PubMed: 23139279]
5. Gonzalez MA, Flynn HW Jr, Smiddy WE, Albini TA, Tenzel P. Surgery for retinal detachment in patients with giant retinal tear: Etiologies, management strategies, and outcomes. Ophthalmic Surg Lasers Imaging Retina. 2013; 44:232–237. [PubMed: 23676223]
6. Ross W, Lavina A, Russell M, Maberley D. The correlation between height of macular detachment and visual outcome in macula-off retinal detachments of ≤7 days' duration. Ophthalmology. 2005; 112:1213–1217. [PubMed: 15921745]
7. Nork TM, Millecchia LL, Strickland BD, Linberg JV, Chao GM. Selective loss of blue cones and rods in human retinal detachment. Arch Ophthalmol. 1995; 113:1066–1073. [PubMed: 7639660]
8. Rex TS, Fariss RN, Lewis GP, Linberg KA, Sokal I, Fisher SK. A survey of molecular expression by photoreceptors after experimental retinal detachment. Invest Ophthalmol Vis Sci. 2002; 43:1234–1247. [PubMed: 11923271]
9. Isernhagen RD, Wilkinson CP. Recovery of visual acuity following the repair of pseudophakic retinal detachment. Trans Am Ophthalmol Soc. 1988; 86:291–306. [PubMed: 2979019]
10. Burton TC. Preoperative factors influencing anatomic success rates following retinal detachment surgery. Trans Sect Ophthalmol Am Acad Ophthalmol Otolaryngol. 1977; 83:OP499–OP505.

11. Tani P, Robertson DM, Langworthy A. Prognosis for central vision and anatomic reattachment in rhegmatogenous retinal detachment with macula detached. Am J Ophthalmol. 1981; 92:611–620. [PubMed: 7304687]
12. Zacks DN, Han Y, Zeng Y, Swaroop A. Activation of signaling pathways and stress-response genes in an experimental model of retinal detachment. Invest Ophthalmol Vis Sci. 2006; 47:1691–1695. [PubMed: 16565410]
13. Matsumoto H, Miller JW, Vavvas DG. Retinal detachment model in rodents by subretinal injection of sodium hyaluronate. J Vis Exp. 2013; 50660
14. Hu R, Chen ZF, Yan J, Li QF, Huang Y, Xu H, Zhang X, Jiang H. Complement C5a exacerbates acute lung injury induced through autophagy-mediated alveolar macrophage apoptosis. Cell Death Dis. 2014; 5:e1330. [PubMed: 25032853]
15. De Hoog VC, Timmers L, Van Duijvenvoorde A, De Jager SC, Van Middelaar BJ, Smeets MB, Woodruff TM, Doevendans PA, Pasterkamp G, Hack CE, De Kleijn DP. Leucocyte expression of complement C5a receptors exacerbates infarct size after myocardial reperfusion injury. Cardiovasc Res. 2014; 103:521–529. [PubMed: 24935433]
16. Miao J, Lesher AM, Miwa T, Sato S, Gullipalli D, Song WC. Tissue-specific deletion of Crry from mouse proximal tubular epithelial cells increases susceptibility to renal ischemia–reperfusion injury. Kidney Int. 2014; 86:726–737. [PubMed: 24850152]
17. Ricklin D, Hajishengallis G, Yang K, Lambris JD. Complement: A key system for immune surveillance and homeostasis. Nat Immunol. 2010; 11:785–797. [PubMed: 20720586]
18. Walport MJ. Complement. First of two parts. N Engl J Med. 2001; 344:1058–1066. [PubMed: 11287977]
19. Walport MJ. Complement. Second of two parts. N Engl J Med. 2001; 344:1140–1144. [PubMed: 11297706]
20. Harboe M, Mollnes TE. The alternative complement pathway revisited. J Cell Mol Med. 2008; 12:1074–1084. [PubMed: 18419792]
21. Guo RF, Ward PA. Role of C5a in inflammatory responses. Annu Rev Immunol. 2005; 23:821–852. [PubMed: 15771587]
22. Langer HF, Chung KJ, Orlova VV, Choi EY, Kaul S, Kruhlak MJ, Alatsatianos M, DeAngelis RA, Roche PA, Magotti P, Li X, Economopoulou M, Rafail S, Lambris JD, Chavakis T. Complement-mediated inhibition of neovascularization reveals a point of convergence between innate immunity and angiogenesis. Blood. 2010; 116:4395–4403. [PubMed: 20625009]
23. Sjöberg AP, Trouw LA, Blom AM. Complement activation and inhibition: A delicate balance. Trends Immunol. 2009; 30:83–90. [PubMed: 19144569]
24. Walsh MC, Bourcier T, Takahashi K, Shi L, Busche MN, Rother RP, Solomon SD, Ezekowitz RA, Stahl GL. Mannose-binding lectin is a regulator of inflammation that accompanies myocardial ischemia and reperfusion injury. J Immunol. 2005; 175:541–546. [PubMed: 15972690]
25. Danese S, Dejana E, Fiocchi C. Immune regulation by microvascular endothelial cells: Directing innate and adaptive immunity, coagulation, and inflammation. J Immunol. 2007; 178:6017–6022. [PubMed: 17475823]
26. Song WC. Membrane complement regulatory proteins in autoimmune and inflammatory tissue injury. Curr Dir Autoimmun. 2004; 7:181–199. [PubMed: 14719381]
27. Song WC, Deng C, Raszmann K, Moore R, Newbold R, McLachlan JA, Negishi M. Mouse decay-accelerating factor: Selective and tissue-specific induction by estrogen of the gene encoding the glycosylphosphatidylinositol-anchored form. J Immunol. 1996; 157:4166–4172. [PubMed: 8892654]
28. Sweigard JH, Yanai R, Gaissert P, Saint-Geniez M, Kataoka K, Thanos A, Stahl GL, Lambris JD, Connor KM. The alternative complement pathway regulates pathological angiogenesis in the retina. FASEB J. 2014; 28:3171–3182. [PubMed: 24668752]
29. Yanai R, Thanos A, Connor KM. Complement involvement in neovascular ocular diseases. Adv Exp Med Biol. 2012; 946:161–183. [PubMed: 21948368]
30. Ambati J, Atkinson JP, Gelfand BD. Immunology of age-related macular degeneration. Nat Rev Immunol. 2013; 13:438–451. [PubMed: 23702979]

31. Hecker LA, Edwards AO, Ryu E, Tosakulwong N, Baratz KH, Brown WL, Charbel Issa P, Scholl HP, Pollok-Kopp B, Schmid-Kubista KE, Bailey KR, Oppermann M. Genetic control of the alternative pathway of complement in humans and age-related macular degeneration. Hum Mol Genet. 2010; 19:209–215. [PubMed: 19825847]
32. Nielsen HE, Larsen SO, Vikingsdottir T. Rate-limiting components and reaction steps in complement-mediated haemolysis. APMIS. 1992; 100:1053–1060. [PubMed: 1492973]
33. Suankratay C, Mold C, Zhang Y, Lint TF, Gewurz H. Mechanism of complement-dependent haemolysis via the lectin pathway: Role of the complement regulatory proteins. Clin Exp Immun. 1999; 117:442–448. [PubMed: 10469045]
34. Nesargikar PN, Spiller B, Chavez R. The complement system: History, pathways, cascade and inhibitors. Eur J Microbiol Immunol. 2012; 2:103–111.
35. Kemper C, Leung M, Stephensen CB, Pinkert CA, Liszewski MK, Cattaneo R, Atkinson JP. Membrane cofactor protein (MCP; CD46) expression in transgenic mice. Clin Exp Immunol. 2001; 124:180–189. [PubMed: 11422193]
36. Harris CL, Rushmere NK, Morgan BP. Molecular and functional analysis of mouse decay accelerating factor (CD55). Biochem J. 1999; 341:821–829. [PubMed: 10417349]
37. Hamilton KK, Ji Z, Rollins S, Stewart BH, Sims PJ. Regulatory control of the terminal complement proteins at the surface of human endothelial cells: Neutralization of a C5b-9 inhibitor by antibody to CD59. Blood. 1990; 76:2572–2577. [PubMed: 1702330]
38. Suzuki H, Lasbury ME, Fan L, Vittal R, Mickler EA, Benson HL, Shilling R, Wu Q, Weber DJ, Wagner SR, Lasaro M, Devore D, Wang Y, Sandusky GE, Lipking K, Pandya P, Reynolds J, Love R, Wozniak T, Gu H, Brown KM, Wilkes DS. Role of complement activation in obliterative bronchiolitis post–lung transplantation. J Immunol. 2013; 191:4431–4439. [PubMed: 24043901]
39. Banadakoppa M, Goluszko P, Liebenthal D, Yallampalli C. Nitric oxide induces segregation of decay accelerating factor (DAF or CD55) from the membrane lipid-rafts and its internalization in human endometrial cells. Cell Biol Int. 2012; 36:901–907. [PubMed: 22574734]
40. Gustafsson DJ, Andersson EK, Hu YL, Marttila M, Lindman K, Strand M, Wang L, Mei YF. Adenovirus 11p downregulates CD46 early in infection. Virology. 2010; 405:474–482. [PubMed: 20638094]
41. Krishnan V, Ponnuraj K, Xu Y, Macon K, Volanakis JE, Narayana SV. The crystal structure of cobra venom factor, a cofactor for C3- and C5-convertase CVFBb. Structure. 2009; 17:611–619. [PubMed: 19368894]
42. Bexborn F, Andersson PO, Chen H, Nilsson B, Ekdahl KN. The tick-over theory revisited: Formation and regulation of the soluble alternative complement C3 convertase ($C3(H_2O)$ Bb). Mol Immunol. 2008; 45:2370–2379. [PubMed: 18096230]
43. Linsenmeier RA, Padnick-Silver L. Metabolic dependence of photoreceptors on the choroid in the normal and detached retina. Invest Ophthalmol Vis Sci. 2000; 41:3117–3123. [PubMed: 10967072]
44. Luo L, Uehara H, Zhang X, Das SK, Olsen T, Holt D, Simonis JM, Jackman K, Singh N, Miya TR, Huang W, Ahmed F, Bastos-Carvalho A, Le YZ, Mamalis C, Chiodo VA, Hauswirth WW, Baffi J, Lacal PM, Orecchia A, Ferrara N, Gao G, Young-Hee K, Fu Y, Owen L, Albuquerque R, Baehr W, Thomas K, Li DY, Chalam KV, Shibuya M, Grisanti S, Wilson DJ, Ambati J, Ambati BK. Photoreceptor avascular privilege is shielded by soluble VEGF receptor-1. Elife. 2013; 2:e00324. [PubMed: 23795287]
45. Lewis GP, Sethi CS, Linberg KA, Charteris DG, Fisher SK. Experimental retinal re-attachment: A new perspective. Mol Neurobiol. 2003; 28:159–175. [PubMed: 14576454]
46. Lewis GP, Talaga KC, Linberg KA, Avery RL, Fisher SK. The efficacy of delayed oxygen therapy in the treatment of experimental retinal detachment. Am J Ophthalmol. 2004; 137:1085–1095. [PubMed: 15183794]
47. Collard CD, Agah A, Stahl GL. Complement activation following reoxygenation of hypoxic human endothelial cells: Role of intracellular reactive oxygen species, NF-κB and new protein synthesis. Immunopharmacology. 1998; 39:39–50. [PubMed: 9667422]

48. Lewis G, Mervin K, Valter K, Maslim J, Kappel PJ, Stone J, Fisher S. Limiting the proliferation and reactivity of retinal Müller cells during experimental retinal detachment: The value of oxygen supplementation. Am J Ophthalmol. 1999; 128:165–172. [PubMed: 10458171]

49. Mervin K, Valter K, Maslim J, Lewis G, Fisher S, Stone J. Limiting photoreceptor death and deconstruction during experimental retinal detachment: The value of oxygen supplementation. Am J Ophthalmol. 1999; 128:155–164. [PubMed: 10458170]

50. Kaczorowski DJ, Scott MJ, Pibris JP, Afrazi A, Nakao A, Edmonds RD, Kim S, Kwak JH, Liu Y, Fan J, Billiar TR. Mammalian DNA is an endogenous danger signal that stimulates local synthesis and release of complement factor B. Mol Med. 2012; 18:851–860. [PubMed: 22526919]

51. Reis ES, Barbuto JA, Isaac L. Human monocyte-derived dendritic cells are a source of several complement proteins. Inflamm Res. 2006; 55:179–184. [PubMed: 16830104]

52. Rutar M, Natoli R, Kozulin P, Valter K, Gatenby P, Provis JM. Analysis of complement expression in light-induced retinal degeneration: Synthesis and deposition of C3 by microglia/macrophages is associated with focal photoreceptor degeneration. Invest Ophthalmol Vis Sci. 2011; 52:5347–5358. [PubMed: 21571681]

53. Ma W, Cojocaru R, Gotoh N, Gieser L, Villasmil R, Cogliati T, Swaroop A, Wong WT. Gene expression changes in aging retinal microglia: Relationship to microglial support functions and regulation of activation. Neurobiol Aging. 2013; 34:2310–2321. [PubMed: 23608111]

54. Ghosh F, Johansson K. Neuronal and glial alterations in complex long-term rhegmatogenous retinal detachment. Curr Eye Res. 2012; 37:704–711. [PubMed: 22578195]

55. Lewis GP, Chapin EA, Luna G, Linberg KA, Fisher SK. The fate of Müller's glia following experimental retinal detachment: Nuclear migration, cell division, and subretinal glial scar formation. Mol Vis. 2010; 16:1361–1372. [PubMed: 20664798]

56. Kaur C, Foulds WS, Ling EA. Blood–retinal barrier in hypoxic ischaemic conditions: Basic concepts, clinical features and management. Prog Retin Eye Res. 2008; 27:622–647. [PubMed: 18940262]

57. Bialas AR, Stevens B. TGF-β signaling regulates neuronal C1q expression and developmental synaptic refinement. Nat Neurosci. 2013; 16:1773–1782. [PubMed: 24162655]

58. Yu J, Liu F, Cui SJ, Liu Y, Song ZY, Cao H, Chen FE, Wang WJ, Sun T, Wang F. Vitreous proteomic analysis of proliferative vitreoretinopathy. Proteomics. 2008; 8:3667–3678. [PubMed: 18752205]

59. Yang L, Bula D, Arroyo JG, Chen DF. Preventing retinal detachment–associated photoreceptor cell loss in Bax-deficient mice. Invest Ophthalmol Vis Sci. 2004; 45:648–654. [PubMed: 14744910]

60. Verardo MR, Lewis GP, Takeda M, Linberg KA, Byun J, Luna G, Wilhelmsson U, Pekny M, Chen DF, Fisher SK. Abnormal reactivity of Müller cells after retinal detachment in mice deficient in GFAP and vimentin. Invest Ophthalmol Vis Sci. 2008; 49:3659–3665. [PubMed: 18469190]

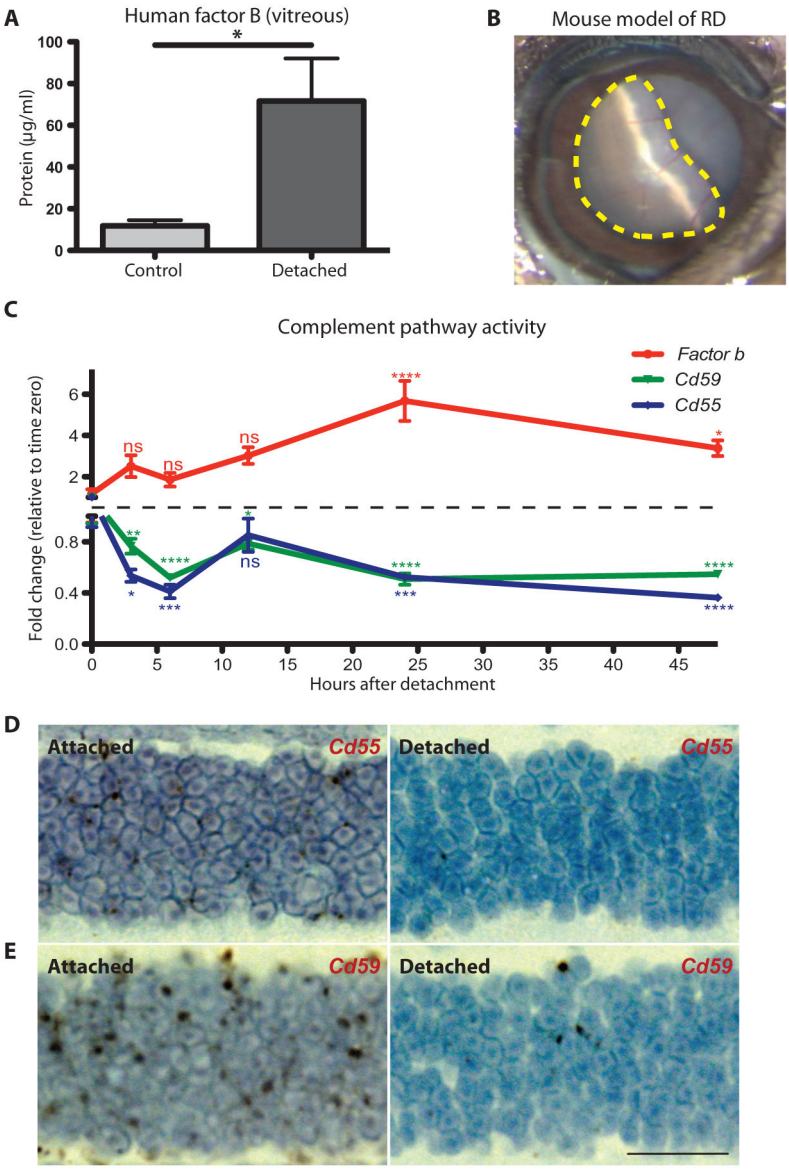

Fig. 1. Activity of the alternative complement pathway during RD

(**A**) ELISA analysis of factor B production in human vitreous from patients with RD (*n* = 10) compared to nondetached retina control patients with a macular hole or epiretinal membrane (*n* = 4). (**B**) Image of RD in a mouse model. The dotted yellow line outlines the region of retina that is detached (about 60%). (**C**) Time course of gene expression for *Fb* (encoding factor B), *Cd55*, and *Cd59* in the retina of mice after RD. The red line tracks *Fb* gene expression, the blue line tracks *Cd55* expression, and the green line tracks *Cd59* expression at intervals over a period of 48 hours. Color of asterisks corresponds to the gene (*n* = 4 for each time point). (**D**) Representative 3,3′-diaminobenzidine labeling (brown) for *Cd55* mRNA expression in the attached outer nuclear layer (left panel) and the detached outer nuclear layer (right panel) of the same eye (*n* = 4). (**E**) 3,3′-Diaminobenzidine labeling (brown) for *Cd59* mRNA expression in the attached outer nuclear layer (left panel) and the

detached outer nuclear layer (right panel) of the same eye ($n = 4$). ns, not significant. *$P \leq 0.05$, **$P \leq 0.01$, ***$P \leq 0.001$, ****$P \leq 0.0001$; unpaired Student's t test. Scale bar, 20 μm.

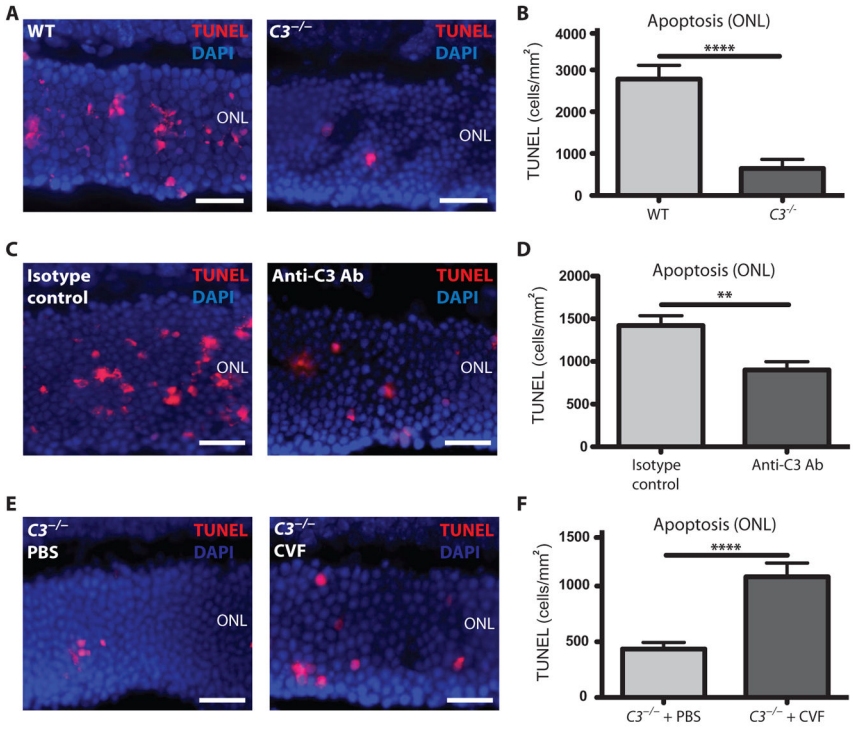

Fig. 2. Apoptosis in complement-deficient mice after RD

(**A**) Representative TUNEL labeling in the outer nuclear layer (ONL) of $C3^{-/-}$ mice and wild-type (WT) control (C57Bl6) mice 24 hours after RD. DAPI, 4′,6-diamidino-2-phenylindole. (**B**) Quantitation of TUNEL cells in the outer nuclear layer of $C3^{-/-}$ mice (n = 8) and WT control mice (n = 8). (**C**) Representative TUNEL labeling in the outer nuclear layer of mice injected with an Ab against C3 compared to injection with an immunoglobulin G (IgG) isotype control Ab. (**D**) Quantitation of TUNEL cells in the outer nuclear layer of mice injected with an Ab against C3 (n = 4) compared to injection with an IgG isotype control Ab (n = 10). (**E**) Representative TUNEL labeling in the outer nuclear layer of $C3^{-/-}$ mice injected with PBS (control) or cobra venom factor (CVF) to activate the complement system. (**F**) Quantitation of TUNEL-positive cells in the outer nuclear layer of $C3^{-/-}$ mice injected with PBS control (n = 5) or cobra venom factor to activate complement in $C3^{-/-}$ mice (n = 8). $^{**}P \leq 0.01$, $^{****}P \leq 0.0001$; unpaired Student's t test. Scale bars, 50 μm.

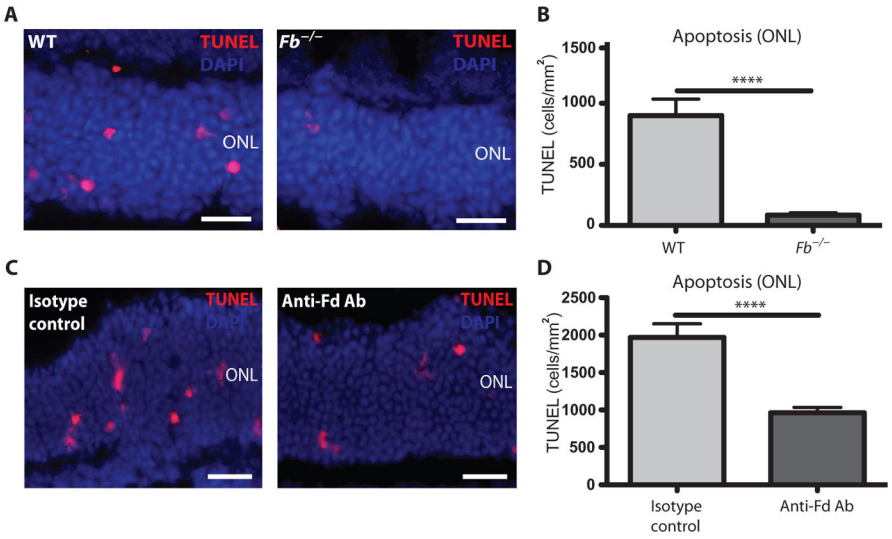

Fig. 3. Apoptosis in alternative pathway–deficient mice after RD

(**A**) Representative TUNEL labeling in the outer nuclear layer 24 hours after RD in mice lacking factor B ($Fb^{-/-}$) and WT control mice. (**B**) Quantitation of TUNEL-positive cells from $Fb^{-/-}$ mice ($n = 6$) and WT control mice ($n = 6$) 24 hours after RD. (**C**) Representative TUNEL labeling 24 hours after RD in mice injected with an anti–factor D (Fd) Ab and IgG isotype control Ab. (**D**) Quantitation of TUNEL-positive cells from mice injected with an anti–factor D Ab ($n = 9$) and IgG isotype control Ab ($n = 9$) 24 hours after RD. ****$P \leq 0.0001$, unpaired Student's t test. Scale bars, 50 μm.

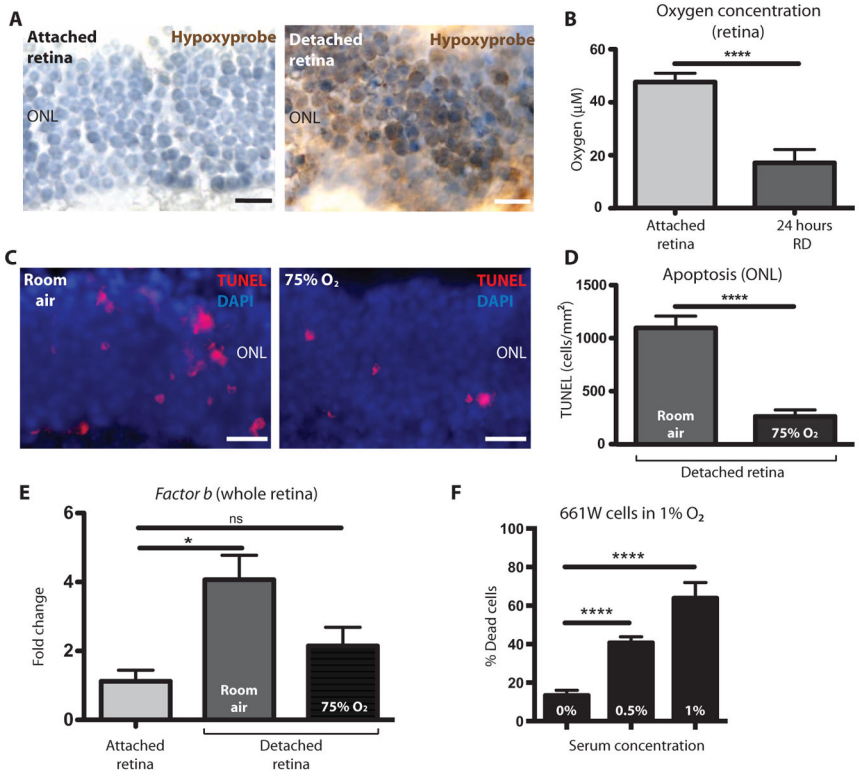

Fig. 4. Hypoxia in the retina after RD

(**A**) Representative immunohistochemistry images of the outer nuclear layer labeled with Hypoxyprobe (brown staining) comparing the detached portion of a mouse retina (right panel) to the attached portion of the same retina (left panel) 24 hours after RD. Both sides of the retina were stained with toluidine blue stain ($n = 7$). (**B**) In vivo oxygen concentrations taken in the retina 24 hours after RD in an attached retina (right eye) compared to the detached retina (left eye) ($n = 7$). (**C**) Representative TUNEL labeling in the outer nuclear layer 24 hours after RD in mice kept in room air (left panel) compared to mice kept in 75% oxygen (right panel). (**D**) Quantitation of TUNEL-positive cells in mice kept in room air ($n = 5$) for 24 hours after RD compared to mice kept in 75% oxygen ($n = 6$). (**E**) RT-PCR showing gene expression for *Fb* (encoding factor B) in the attached or detached retina 24 hours after RD; comparing mice kept in room air to mice kept in 75% oxygen (attached, $n = 3$; room air, $n = 3$; 75% O_2, $n = 4$). (**F**) Under hypoxic conditions (1% O_2), increasing mouse serum concentrations (used as a source of complement) led to an increased percentage of cell death in 661W cells assessed using a live/dead assay ($n = 4$). $^*P \leq 0.05$, $^{****}P \leq 0.0001$; unpaired Student's *t* test. Scale bars, 50 μm.